

## FUZZY SEGMENTATION OF SAR IMAGES FOR OIL SPILL RECOGNITION

A. Barni <sup>(1)</sup>, M. Betti <sup>(2)</sup>, A. Mecocci <sup>(3)</sup>

<sup>(1)</sup> Università degli Studi di Firenze, Italy

<sup>(2)</sup> Università degli Studi di Perugia, Italy

<sup>(3)</sup> Università degli Studi di Pavia, Italy

**Abstract** - A three-step algorithm is developed to segment oil spills from a marine background on Synthetic Aperture Radar (SAR) data. First, filtering is performed to reduce speckle noise. Then fuzzy clustering is carried out to obtain a preliminary partition of the pixels on the basis of their grey level intensities. A very simple cluster validity criterion is tested to determine the optimal number of clusters present in the data. In order to improve segmentation a final step involves a cluster merging procedure using edge information provided by a Sobel operator. The algorithm has been tested on SEASAT images.

### 1. INTRODUCTION

Despite its short life, SEASAT has shown that radar technology can be exploited for a great deal of applications: among other capabilities, the importance of radar sensors in detection and surveillance of oil pollution has been established, (Bern et al. (1)). Off-shore oil and gas exploration and production in areas with extreme weather conditions have increased the probability of severe environmental damage due to oil spills. Extended ocean monitoring could reduce potential damage through improving efficiency of clean-up operations and reducing deliberate pollution, e.g. bilge pumping at sea.

In general, marine pollution is accompanied by formation of surface films: their thermodynamical properties are substantially different from those of pure water, and cause sensible effects in e.m. radiation transfer through the interface, which can be sensed by radars as variations of backscattering coefficient  $\sigma^0$ . Backscattering behaviour can be explained by considering marine surface as rough, made up of long gravitational waves with capillary waves superimposed. It has been shown that a resonance condition exists (Bragg's condition), according to which only waves with certain frequencies cause radiation to be backscattered.

The presence of an oil layer on sea surface causes a significant damping of the capillary wavelengths (Bern et al (1)), resulting in an evident ocean backscatter depression (3-13 dB, depending on polarization). Visibility of the slick depends upon local wind conditions, being it possible only for a limited range of wind speeds, and it is best on images acquired from radar sensors operating with VV-polarization.

The problem dealt with here is detecting oil spills on sea surface through a three-step segmentation procedure. A non-linear filter is applied to reduce

speckle noise: in order to select the most suitable filter a comparison among several speckle filtering techniques has been accomplished; then fuzzy clustering is performed, producing a preliminary partition of the image. The fuzzy approach has been chosen for its ability to deal with complex situations such as cover class mixture and vague boundaries among regions, quite commonly found in remote sensing images. Lastly, an edge-driven cluster merging technique is carried out to refine the segmentation obtained from the previous step. The effectiveness of the algorithm has been tested on SEASAT images (Fig. 1), but it would work the same with any radar image.

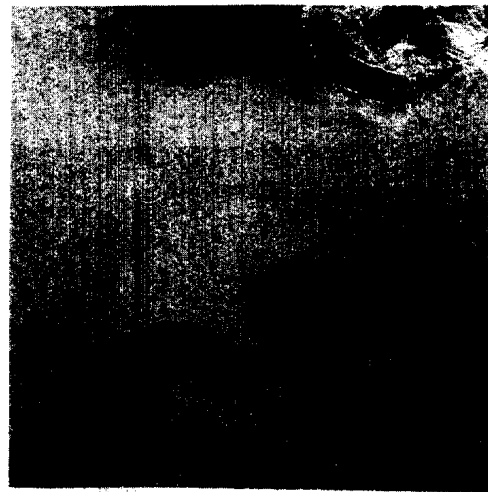


**Figure 1** - SEASAT image used to test the effectiveness of the proposed algorithm.

### 2. FILTERING

SAR images are affected by speckle noise. Basically, speckle noise has the nature of multiplicative noise (Ulaby et al. (2)):

$$Z = x \cdot u \quad (1)$$

where  $z$  is the intensity of an observed pixel,  $x$  is the noise-free pixel, and  $u$  is the noise. This is the main problem in SAR images interpretation, since even a zone that is homogeneous on the ground has a granular

aspect and a statistical distribution with a large standard deviation. Therefore the first step of the processing chain consists of a filtering operation. Six different filters of two groups have been compared: the first group comprises box, median and geometric filters, which are general noise-reducing filters and do not assume any *a priori* speckle model; the second group is composed by sigma, Lee and Kuan filters, which are adaptive filters assuming for speckle a multiplicative model.

Box (or average) and median filters are the simplest ones, replacing each point with the mean or median value of a given window. The others deserve a separate discussion.

### Geometric Filter

It was introduced by Crimmins (3), and it is an iterative algorithm which has the effect of reducing the undesired speckle noise while preserving the edges of the original image. Noise reduction is accomplished by applying a complementary hulling technique to the image *umbra*. The algorithm works by recursively smoothing peaks and filling valleys of the umbra, which leads to speckle reduction. Peaks wider than a certain threshold are not reduced, thus preserving strong radar returns. A detailed description of Geometric Filter can be found in Crimmins (3).

### Sigma Filter

Sigma filter has been developed by Lee (4). It works like box filter, but it assumes a multiplicative noise model: given a  $n \times n$  window, sigma filter does not use all  $n^2$  pixels of the window to compute the mean value, but only those whose grey level is within the range  $[(1-2C_u)z, (1+2C_u)z]$ , where  $z$  is the centre pixel value, and  $C_u$  is the noise coefficient of variation, whose value can be computed theoretically once the image type is given, (Ulaby et al. (2)).

### Lee Filter

Lee filter, (Lee (5)) uses a quadratic criterion that minimizes  $E\{(x' - x)^2\}$  for each pixel value, where  $x'$  is the estimated value of  $x$ . It makes the assumption that noise is additive with a mean value equal to zero. Having a multiplicative speckle, the solution involves a logarithmic transformation before filtering and an exponentiation after it.

It can be seen, (Lee (5)), that the best linear estimate is:

$$x'(i, j) = z(i, j) \cdot w(i, j) + \bar{z}(i, j) \cdot [1 - w(i, j)] \quad (2)$$

where the weighting function  $w$  is given by:

$$w(i, j) = 1 - \frac{C_u^2}{C_z^2} \quad (3)$$

$C_u$ , as before, is the noise variation coefficient, and  $C_z = \sigma_z / \bar{z}$  is the local variation coefficient, with  $\sigma_z$  and  $\bar{z}$  standard deviation and mean value computed over a window of a given size.

### Kuan Filter

It uses the same quadratic criterion of Lee Filter, (Kuan et al. (6)), but here the assumption is that noise is multiplicative with a mean value of one. In this case we obtain for  $x'$  the same expression (3), but the weighting function becomes:

$$w(i, j) = \left(1 - \frac{C_u^2}{C_z^2}\right) / (1 + C_u^2) \quad (4)$$

Tests have been performed to assess filters effectiveness: for filters using a moving window (box, median, sigma, Lee and Kuan filters) a window of size  $7 \times 7$  was chosen, while 5 iterations were used for geometric filter. The box, median and geometric filters work quite well, but causing a certain loss of texture information (especially geometric filter), which could be detrimental to interpretation purposes; this is not true for sigma, Lee and Kuan filters, which give very similar results (especially Lee and Kuan filters, whose grey level histograms can be shown to be almost identical); hence, at this stage, only Lee filter was discarded.

Final selection of *best* filtering technique has been based upon performance of the overall segmentation chain. As it will be shown in Section 5, sigma and Kuan filters grant best results.

## 3. CLUSTERING

Traditional (hard) clustering assigns each data point to one and only one cluster, assuming well defined boundaries between clusters. This can't be the case for remote sensing images, where each pixel corresponds on the ground to a cell of tens of square meters, which quite often contains a mixture of surface-cover classes; in addition, boundaries among regions are hardly ever sharp. Fuzzy set theory (Bezdek (7)) provides useful concepts and tools to cope with this sort of problems: here a *membership function*  $u_A(x)$  is assigned to each pixel  $x$ , which measures "how much" the pixel belongs to the set  $A$ , with  $u_A(x)=0$  meaning no membership,  $u_A(x)=1$  full membership, and  $u_A(x) \in ]0,1[$  partial membership. Interpreting cover classes as fuzzy sets allows to deal with complex situations such as cover mixture or intermediate conditions, since each pixel can have partial membership in more than one class, although it can't completely belong ( $u_A(x)=1$ ) to more than one.

Bezdek, (Bezdek (7)) developed a family of clustering algorithms based on a fuzzy extension of the least-square error criterion. The one used in this work is the

c-means algorithm (FCM), which is based on the minimization of the following objective function:

$$J_m(U, V) = \sum_{k=1}^n \sum_{i=1}^c (u_{ik})^m \|x_k - v_i\|^2 \quad (5)$$

where  $X = \{x_1, x_2, \dots, x_n\}$  is the data set,  $V = \{v_1, v_2, \dots, v_c\}$  is the set of prototypes (cluster centers),  $u_{ik} \in U$  is membership value of point  $x_k$  in cluster  $v_i$  and  $m$  controls the *fuzziness* of the clusters.

Fuzzy partition is carried out through an iterative optimization of expression (5). Once the fuzzy partition is obtained, a clustering map is produced by assigning each pixel to the cluster to which it mostly belongs.

A final operation involves median post-filtering of the map to obtain more homogeneous regions.

FCM algorithm has been implemented in two different forms: the first one directly on the image, and the second one on a pyramid structure obtained from the image itself: a pyramid (Trivedi and Bezdek (8)) is created by averaging groups of pixels in a neighbourhood to produce a new composite pixel of reduced resolution, and thus a low resolution image with fewer pixels. This process is repeated on the processed image to form a new image of lower resolution (and fewer pixels) still.

The c-means procedure is implemented initially on the upper levels of the pyramid (8); a test is carried out, for each pixel  $x_k$ , on the final membership values:

$$\max\{u_{1k}, u_{2k}, \dots, u_{ck}\} \geq T \quad (6)$$

where  $T$  is a prescribed threshold. If condition (6) is not verified the pixel is labelled as *uncertain*; the clustering procedure is then repeated on all uncertain pixels at the lower level, higher resolution, image. In this way the algorithm works on a very limited number of points each time, and computation time can be reduced by a large amount.

The main difficulty encountered when clustering real data is that number of clusters  $c$  can not always be defined a priori, and one has to find a validity criterion, in order to determine the optimal number of clusters present in the data.

The mathematical validity index chosen as a performance measure of the clustering procedure is the Partition Coefficient  $F$  (Bezdek (7)), defined as:

$$F(U; c) = \frac{1}{n} \sum_{k=1}^n \sum_{i=1}^c u_{ik}^2 \quad (7)$$

which can be interpreted in terms of the amount of *overlap* in pairwise intersections of the  $c$  fuzzy subsets in partition  $U$ ; computing the parameter  $F$  for various numbers of clusters  $c$ , a relative maximum for  $c=c^*$  can be interpreted as the image having a probable *optimum* number of classes equal to  $c^*$ .

#### 4. CLUSTER MERGING

A third step in the segmentation procedure is necessary since the number of regions identified by fuzzy clustering is normally too large. Typically, SAR images present grey level variations along the range direction, due to increasing incident angle of radiation, so that even homogeneous regions (e.g. water bodies) are split into different clusters. A merging criterion needs to be used in order to reduce the number of regions: the first operation involves identifying the connected regions in the clustering map; in parallel a thresholded Sobel operator is applied to enhance the main edges of the original filtered image; lastly, those regions whose common boundaries do not present a high enough percentage of large gradient points are merged together.

#### 5. RESULTS AND CONCLUSIONS

The complete algorithm has been implemented on a 80486 DX2 personal computer using IDL, a software for analysis and display of digital data.

The pyramidal c-means procedure has been preferred to the traditional one, since it combines comparable or better results to a considerably shorter computation time. Parameters  $m$  and  $T$  were set to 2 and 0.985 respectively; the topmost level of the pyramid was set to  $32 \times 32$ , while the bottom one was  $128 \times 128$ , in order to achieve fast clustering.

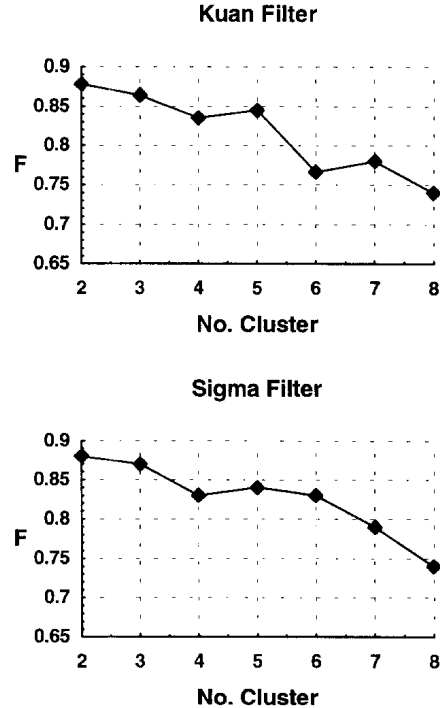
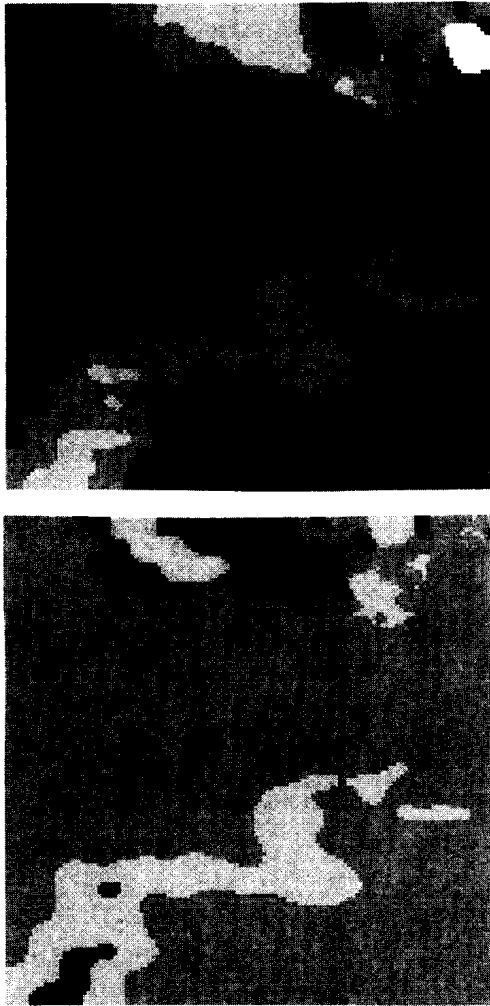


Figure 2 - Partition coefficient  $F$  vs. the number of clusters. The optimum number is  $c = 5$ .

As far as the number of clusters is concerned, the parameter  $F$  shows a relative maximum for  $c=5$  in most cases, as it can be seen in Fig. 2 for the special case of images processed with sigma and Kuan filters.

Fig. 3 shows the relative clustering maps, while in Fig. 4 we have the final results of the segmentation procedure, with boundaries among regions enhanced and superimposed to the original filtered images: we can see that the contour of the oil slick is well evident, even though it is still split into two clusters: the inner part of the slick, where the oil film is thicker, is considerably darker, and the algorithm considers it as another region; land keeps instead to be split into many different clusters.



**Figure 3** - Clustering maps obtained by starting from the images filtered with sigma (top) and Kuan filters (bottom)

The experimental results shown demonstrate the validity of the algorithm proposed to segment oil spills from the background: in particular, the filters having a

certain a priori knowledge of the speckle phenomenon seem to provide better results, as it is expected; sigma filter, being the fastest, could be preferred for very large dimensions images, where processing time required using Lee or Kuan filters might become prohibitive. Despite its simplicity coefficient  $F$  seems to work well as a validity criterion.

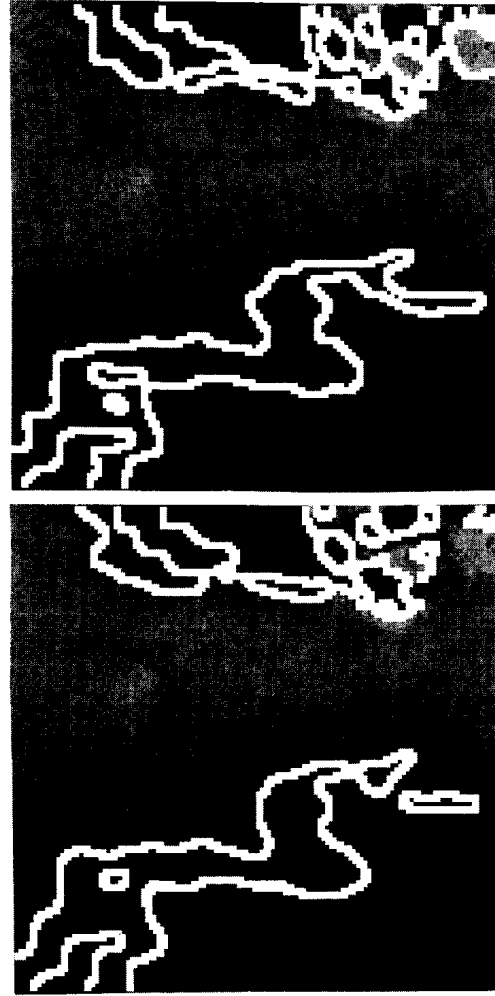


**Figure 4** - Final results of the segmentation procedure. The top image refers to the sigma filter case, while the one on the bottom has been obtained by using a Kuan filter.

Sobel gradient is a fast edge-enhancing algorithm, but can't probably allow optimal results; new edge detectors have been developed for the specific case of SAR images (Touzi et al (10)), and their use could sensibly improve the cluster merging technique.

As it has been said it is the damping of ocean ripples due to a mineral oil film on marine surface to allow slick detection: nevertheless, such damping may be caused by a number of other natural mechanisms (remnants of internal wave trains near a coast,

biological activity, fresh water run-off, etc.), and it is difficult, at present, to make an unambiguous distinction among these different phenomenon. It seems, however, that a chance to discriminate between monomolecular and multimolecular oil films exists using multi-frequency sensors (Alpers and Hühnerfuss (9)); otherwise, another possibility could be the creation of new synthetic bands, e.g. exploiting texture information, which could be different enough between water and oil: in particular, fractal models (Steward et al (11), Werman and Peleg (12)) are frequently being used for image segmentation, even if extreme care must be taken in choosing the "fractal signature" used to characterize the regions of the image.

## REFERENCES

1. Bern T.I., Wahl T., Anderssen T., Olsen R., New Orleans, LA, 15-17 June 1992, "Oil Spill Detection Using Satellite Based SAR: Experience from a Field Experiment", First Thematic Conference on Remote Sensing for Marine and Coastal Environments
2. Ulaby F.T., Kouyate F., Brisco B., Lee Williams T.H., 1986, "Textural Information in SAR images", IEEE Trans. Geosci. Remote Sensing, vol. GE-24, no. 2, 235-245
3. Crimmins T.R., 1985, "Geometric Filter for Speckle Reduction", Applied Optics, vol. 24, no. 10, 1438-1443
4. Lee J.S., 1983, "A Simple Speckle Smoothing Algorithm for Synthetic Aperture Radar Images", IEEE Trans. Syst. Man Cybern., vol. SMC-13, no. 1, 85-89
5. Lee J.S., 1980 "Digital Image Enhancement and Noise Filtering by Use of Local Statistics", IEEE Trans. Pattern Analysis Machine Intelligence., vol. PAMI-2, no. 2, 165-168
6. Kuan D.T., Sawchuck A.A, Strand T.C. and Chavel P. 1985 "A Noise Smoothing Filter for Images with Signal-Dependent Noise", IEEE Trans. Pattern Analysis Machine Intelligence, vol. PAMI-7, no. 2, 165-177.
7. Bezdek J.C., 1981, "Pattern Recognition with Fuzzy Objective Function Algorithms", Plenum Press
8. Trivedi M.N., Bezdek J.C., 1986, "Low-Level Segmentation of Aerial Images with Fuzzy Clustering", IEEE Trans. Syst. Man Cybern., vol. SMC-16, no. 4, 589-598
9. Alpers W.R., Hühnerfuss H., 1998, "The Damping of Ocean Waves by Surface Films: a New Look at an Old Problem", J. Geophys. Res. 94, C5, 6251-6265
10. Touzi R., Lopes A., Bousquet P., 1988, "A Statistical and Geometrical Edge Detector for SAR Images", IEEE Trans. Geosci. Remote Sensing, vol. GE-26, no. 6, 764-773
11. Steward C.V., Moghaddam B., Hintz K.J., Novak L.M., 1993, "Fractional Brownian Motion Models for Synthetic Aperture Radar Imagery Scene Segmentation", Proceedings of the IEEE, vol. 81, no. 10, 1511-1522
12. Werman M., Peleg S., 1985, "Min-Max Operators in Texture Analysis", IEEE Trans. Pattern Anal. Mach. Intell., vol. PAMI-7, no. 6, 730-734